Tetiaroa diachronic geomorphology 1955 -2023 Monitoring the shoreline and vegetation cover of tropical atoll in the climate change context

Benoît Stoll, Tobias Fischer, Julie Daniellot-Dejoux, Marania Hopuare

Tetiaroa diachronic geomorphology 1955 – 2023
Monitoring the shoreline and vegetation cover of a tropical atoll in the climate change context

Benoît Stoll[1 3], Tobias Fischer[1], Julie Daniellot-Dejoux, Marania Hopuare[2]

[1] UMR 241 SECOPOL – University of French Polynesia

[2] GePaSud lab. – University of French Polynesia

[3] Corresponding author: benoit.stoll@upf.pf

Abstract:

The Tetiaroa atoll is virtually free of anthropogenic pressure, making it a textbook case for observing the impact of climate change on the pristine coral atolls of French Polynesia.

A geospatial database dating back to 1955 was used to map and analyze erosion and accretion phenomena on the atoll's *motu* (Tahitian name for islets).

Its diachronic analysis documents two types of *motu*: those with a coralline base, which experience minimal movement over time, and the sandy *motu* which, on the contrary, exhibit significant dynamics linked to strong swells and storms.

While we cannot yet link the observed dynamics to climate change and rising sea levels, these results will help us better understand the future impacts of extreme climatic events on Polynesian atolls.

1. Introduction

1.1. The study area and database

Tetiaroa island is a 33.8 km^2 coral atoll, located at 17°00'S, 149°34'W, 50 km north of Tahiti in French Polynesia (FIGURE 1). Originally consisting of 13 islets (*motu* in Tahitian), one of them, *Motu One*, disappeared between 1955 and 1981.

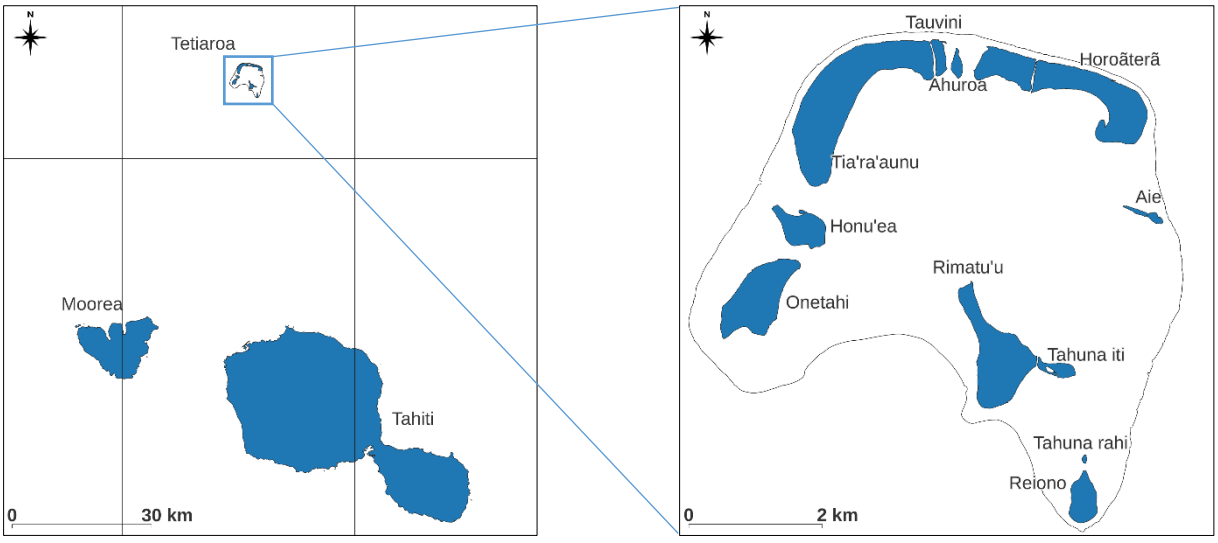

FIGURE 1. Tetiaroa atoll location in Windward Archipelago - French Polynesia

The atoll has been privately owned since it was given to Johnston Walter Williams in 1904 by the Tahitian royal family. Williams initiated massive copra cultivation across the atoll's islets, but coconut plantations were apparently already present, probably planted by previous owners. In 1967, the atoll was sold to Hollywood actor Marlon Brando, who abandoned the coconut plantations and left the islet's forests to slowly renaturalize.

Tetiaroa is therefore a textbook case of a coral atoll that has undergone very little human activity or impact for almost 60 years; the islet of Onetahi is the only one to have undergone significant human activity. In accordance with Marlon Brando's wishes, Tetiaroa has become an open-air laboratory for environmental conservation and can be considered an ideal place to study the impacts of global warming on non-anthropogenic coral atolls.

Since the creation of the Tetiaroa Society in 2014, a database of very high resolution remotely sensed images dating back to 1955 has been compiled for the atoll (TABLE 1). This database is constantly being enriched with new VHR satellite images as often as possible.

Date	Type	Sensor	Specs	Rights
1955	*Aerial Orthophoto*	*B&W*	*1.2m*	*DAF TOPO - PF*
1981	*Aerial Orthophoto*	*B&W*	*1m*	*DAF TOPO - PF*
2001	*Aerial Orthophoto*	*Color*	*0.5m*	*DAF TOPO - PF*
2004	*Aerial Orthophoto*	*Color*	*0.8m*	*DAF TOPO - PF*
2010	*Satellite image*	*Worldview2*	*0.5m, 8 bands*	*DAF TOPO - PF*
2012	*Satellite image*	*Worldview2*	*0.5m, 8 bands*	*GePaSud Lab - UPF*
2014	*Satellite image*	*Pléiades*	*0.7m, 4 bands*	*UTH Zurich - IDEA*
2016	**Satellite image**	**Pléiades**	**0.5m, 4 bands**	**GePaSud Lab - UPF**
2017	**Helicopter born**	**Lidar**	**25 dots/m^2**	**UTH Zurich - IDEA**
2019	**Satellite image**	**Pléiades**	**0.5m, 4 bands**	**GePaSud Lab - UPF**
2020	**Satellite image**	**Worldview3**	**0.3m, 4 bands**	**DAF TOPO - PF**
2022	**Satellite image**	**Pléiades**	**0.5m, 4 bands**	**TETIAROA SOCIETY**
2023	**Satellite image**	**Pléiades**	**0.5m, 4 bands**	**GePaSud Lab - UPF**

TABLE 1. *Historical Tetiaroa raster database (**previously unprocessed data in bold**)*

1.2. Previous studies on Tetiaroa motu geomorphology

A previous study (Le Cozannet et al., 2013) mapped the shoreline of the Tetiaroa islets on aerial photographs from 1955, 1981 and 2001. (Stoll and Longine, 2019) has extended this study to map land use in 6 terrestrial and intertidal classes as well as the *motu* shorelines using images from 1955 to 2014 (italic in TABLE 1).

This study also considers a 1907 notarial document listing all the *motu* surfaces on Tetiaroa. These surfaces are extracted from a legal document, the measurements were taken by a professional surveyor, and they can be considered relatively accurate since they show almost no discrepancies with the surfaces extracted from the various historical aerial and satellite images (FIGURE 13 and TABLE 2). The only exception is *Tia'ra'aunu*, which is 40 ha larger than in 1955; this could be a transcription, or a measurement error exacerbated by the vastness of the *motu*'s surface area.

This article aims to reconsider the diachronic analysis of the geomorphology of Tetiaroa's islets on an updated database by adding unprocessed remote sensing data such as very high-resolution satellite images from 2016 to 2023 and 2017 lidar data (bold in TABLE 1).

2. Geomatic processing

2.1. Shoreline indicators

The French Navy's hydrographic and oceanographic service (SHOM) defines the shoreline as the intersection between land and sea at high tide (tidal coefficient 120) under normal meteorological conditions. However, measuring the shoreline in the field is challenging: (Boak and Turner, 2005) identified 43 shoreline indicators. However, some indicators seem more relevant than others, depending on the case studied. Here, we have selected two indicators: the vegetation boundary and the instantaneous shoreline.

The vegetation limit corresponds to the "outer limit of the densest vegetated zones developing on the emerged and stabilized parts of coral islands and coastal sedimentary systems" (Pillet, 2020). It is relatively stable in nature but does not consider variations in beaches and other intertidal zones, thus does not allow a good approximation of the *motu* surfaces.

The instantaneous shoreline limit is the position of the land/water interface at a given moment (Boak and Turner, 2005) and has the advantage of taking intertidal spaces into account and being a closest approximation of the shoreline. This method is often used to study atolls in general (Le Cozannet et al., 2013; Stoll and Longine, 2019; Yates et al., 2013).

However, it is highly sensitive to tidal variations, as well as seasonal variations in beaches and sandbanks. The shoreline should therefore be assessed over longer time intervals to consider the tidal cycles (*ibid.*) or require tidal corrections.

Tidal correction is out of reach on most of the satellite images in the Tetiaroa database due to the absence of concomitant 3D beach models (although satellite coastal bathymetry has not yet been considered), but also due to the absence of tide gauge data inside the Tetiaroa lagoon. Indeed, even if tide gauge data are available on the nearby island of Tahiti, Tetiaroa is a closed atoll (i.e. with no major pass) and the water level inside the lagoon is different from that outside, due to the damping phenomenon of filling/emptying.

On the other hand, Tetiaroa is located close to an amphidromic point (Botella, 2015; Canavesio, 2019; Dumas et al., 2012) which leads to low tidal coefficients inside the lagoon of Tetiaroa and reduce the impact of tidal errors, making the instantaneous shoreline more accurate and relevant.

2.2. Extracting shoreline indicators from satellite images

2.2.1. Vegetated zone

The vegetated part of the *motu* serves as a good indicator of the *motu*'s geomorphology, as long as it is fully vegetated, which is the case in Tetiaroa.

The vegetated area is extracted using the widely used Normalized Difference Vegetation Index (NDVI) (Kriegler et al., 1969).

$$NDVI = (NIR - R)/(NIR + R) \quad (1)$$

2.2.2. Instantaneous shoreline

The Normalized Difference Water Index (NDWI) (Gao, 1996) is a classic remote sensing tool for locating shoreline on multispectral satellite images (using the near infrared band).

$$NDWI = (G - NIR)/(G + NIR) \quad (2)$$

For this study, we used the new Direct Difference Water Index (DDWI) (Abdelhady et al., 2022).

$$DDWI = G - NIR \quad (3)$$

In (Abdelhady et al., 2022), the DDWI was applied to several types of satellite images (PlanetScope, Sentinel, RapidEye) of Lake Michigan in the USA, for the purpose of comparison. The highest spatial resolution studied was 3 meters, and the present study is the first attempt to apply this index to a tropical island territory using Pleiades, Worldview2 and Worldview3 satellite images with 70cm, 50 cm and 30 cm spatial resolutions.

Empirical comparisons (FIGURE 2) between NDWI (EQ. 2) and DDWI (EQ. 3) have shown that the difference in shorelines extracted using these two indexes has more to do with the choice of image segmentation threshold and cleaning protocol than with the index itself. This point will be studied in greater detail in a subsequent publication. The DDWI has been used throughout this study.

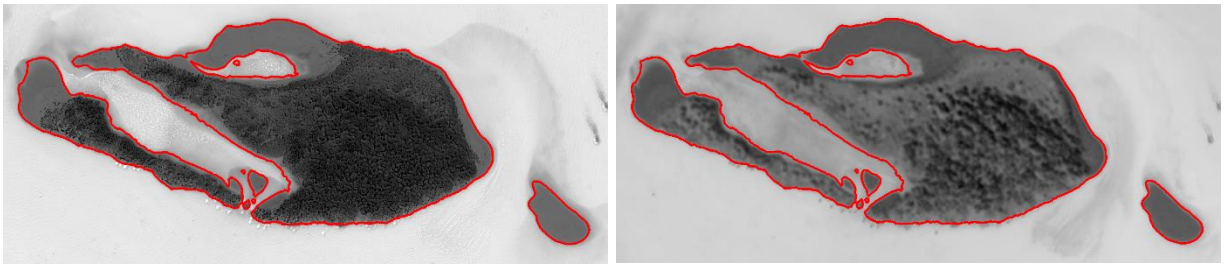

FIGURE 2. NDWI (left), DDWI (right) and extracted shoreline (red line) of Tahuna iti (2016 Pléiades)

2.2.3. Processing the NDVI and DDWI

In both cases, the QGIS processing chain is identical: (i) apply the formula (EQ 1 or 3) to the satellite image bands using a raster calculator, (ii) threshold the resulting raster using (EQ 4), (iii) transform the raster into a vector, (iv) clean up the vector in order to obtain clean polygon vectors as shown in (FIGURE 3). This manual vector cleaning step is the most time-consuming, as the resulting "emerged part" polygon vectors must be unique for each *motu*, and free from holes and vector topology errors. On the other hand, the polygon vectors of the "vegetated part" can be multiple but must also be free of holes and topology errors.

All the above processes are carried out using simple raster and vector GIS tools.

$$INDEX_{BIN} = INDEX > THRESHOLD \quad (4)$$

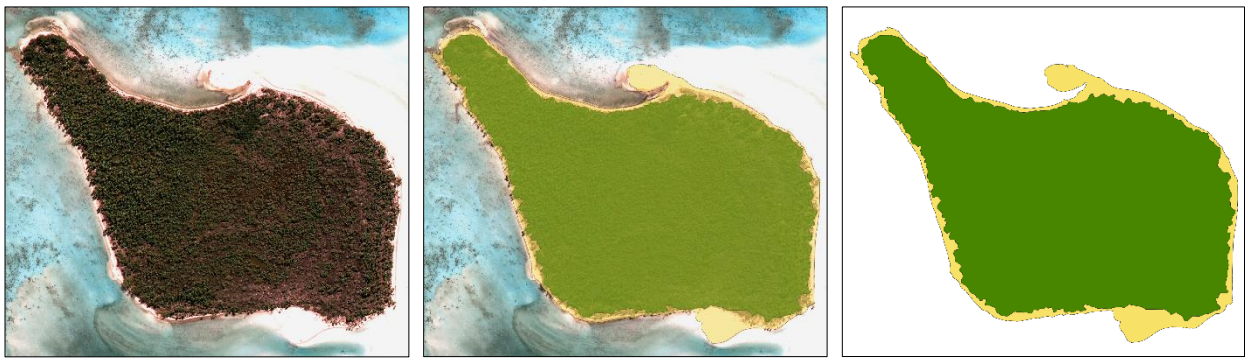

FIGURE 3. Emerged part (DDWI-yellow) and vegetated part (NDVI-green) of Honu'ea motu

2.3. Other shoreline indicators digitalization methods

2.3.1. dGPS instantaneous shoreline digitalization

Very high-resolution satellite images are hard to get in tropical areas due to the persistent cloud cover all year long, and regular dGPS shoreline digitalization (post-processed Trimble Geo7X – 2

cm accuracy) are carried out along the 47km shoreline to better understand seasonal variations and fill in potential gaps in satellite acquisitions.

2.3.2. Photointerpretation of Aerial orthophotography

Photointerpretation can provide the same results (emerged and vegetated areas polygons) from aerial orthophotography, provided they have been registered correctly. This was done in (Stoll and Longine, 2019) using shallow coral patches in the lagoon as permanent landmarks.

2.3.3. Processing lidar data

Lidar data is very different from the other image types (aerial and satellite images), as it involves a 25 dots/m^2 3D point cloud instead of raster images. Basic lidar processing (lastools software) of the raw point cloud provides an emerged land raster image whose pixels represent the presence/absence of points above 0 m (out of the water). Vegetated areas were extracted from a 5-stratum vegetation model processed in (Stoll et al., 2023), retaining all areas containing information on one or more vegetation strata.

2.4. Characterizing the islets morphodynamic

Of the 13 images in the 1955-2023 database (TABLE 1), each of the 3 main data types was processed using appropriate methods: photointerpretation of aerial orthophotography, specific lidar processing based on a point cloud for lidar data, and radiometric indexes (NDVI and DDWI) for satellite images. The resulting database consists of 26 polygon vector files (emerged and vegetated vectors for each image).

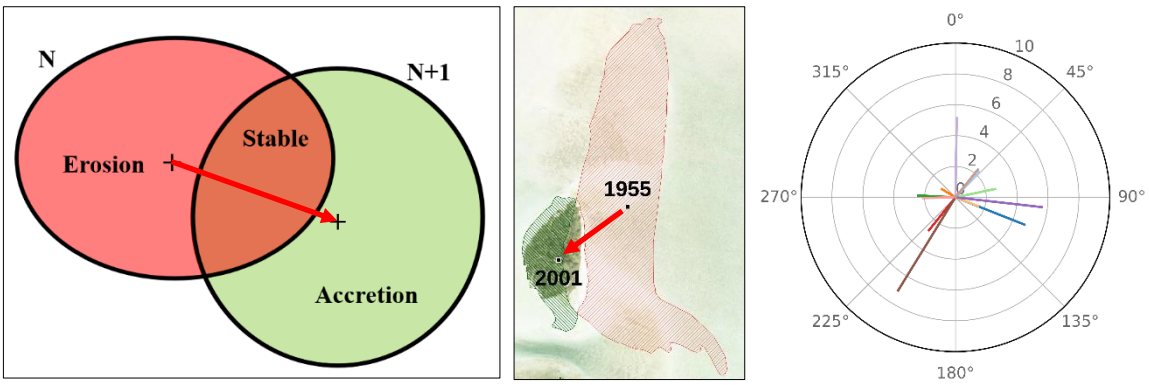

FIGURE 4. Erosion, accretion and centroid displacement between consecutive polygon vectors (N and N+1).

$$Accretion = (N+1) - (N) \quad (3)$$

$$Erosion = (N) - (N+1) \quad (4)$$

$$Stable = (N+1) - Accretion = (N) - Erosion \quad (5)$$

Unlike the analysis of linear shorelines (as, for example, on the Atlantic coast of France), atoll islets are spatially finite with closed shorelines. Once mapped, they can be represented by polygon vectors instead of linear ones. In this way, simple vector tools can calculate the size (area) and dynamics (erosion, accretion, shoreline or centroid movement) of these polygons, enabling a complete diachronic analysis.

There are several methods for characterizing the geomorphology of a *motu*, the simplest being single-date indexes such as (i) the emergent surface for each date and (ii) the vegetated surface for each date. But these single-date indexes do not represent *motu* dynamics with sufficient accuracy.

Multi-date indexes must also be considered, such as erosion surfaces, accretion surfaces and centroid movements. The mapping of erosion and accretion between two dates (i.e. between two polygons) is obtained by simple vector operations (FIGURE 4 and EQ 3,4,5). See (TABLE 2) for full single-date and multi-date surfaces report.

Monitoring *motu* dynamics must also consider the movement between each consecutive polygon centroid (Albert et al., 2016; Paris and Mitasova, 2014). The centroid is calculated for each *motu* using conventional polygon vector tools, then the distance and azimuth between the two consecutive centroids are processed using the QGIS field calculator. A polar diagram (FIGURE 4 right) highlights the *motu's* various movements in direction and distance; see (FIGURE 16) for full reports.

3. Diachronic analysis

Superimposing polygon vectors of the shorelines from 1955 to 2023 (FIGURE 5) highlights stable and unstable zones. Two types of *motu* are present on Tetiaroa: most are stable (appear blue in FIGURE 5) with a few shifting sandy spires (circled in orange and green in FIGURE 5), and a few are highly dynamic (circled red in FIGURE 5).

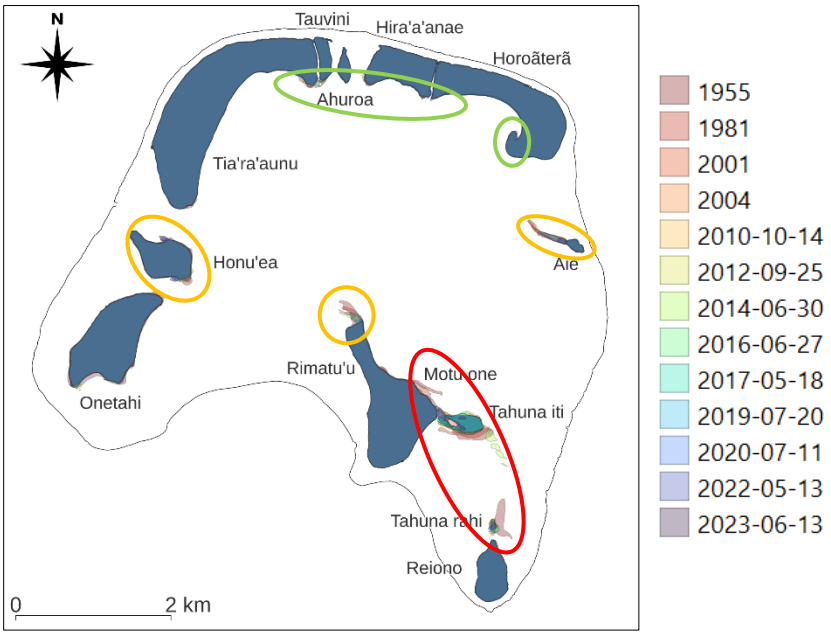

FIGURE 5. Shoreline overview: stable (blue), sandy spires (orange and green) and dynamic sand bank area (red)

3.1. Stable motu

Stable areas are *motu* that have remained unchanged throughout the database period, except for a few sandy spires.

This applies to 10 out of 13 *motu*: *Reiono, Rimatu'u, Onetahi, Honu'ea, Tia'ra'aunu, Tauvini, Ahuroa, Hira'a'anae, Horoāterā, Aie*. All these *motu* show very little change in their emergent or vegetated surfaces between 1955 and 2023, and the areas of erosion and accretion are quite small, as in the example of *Honu'ea* (FIGURE 6 left).

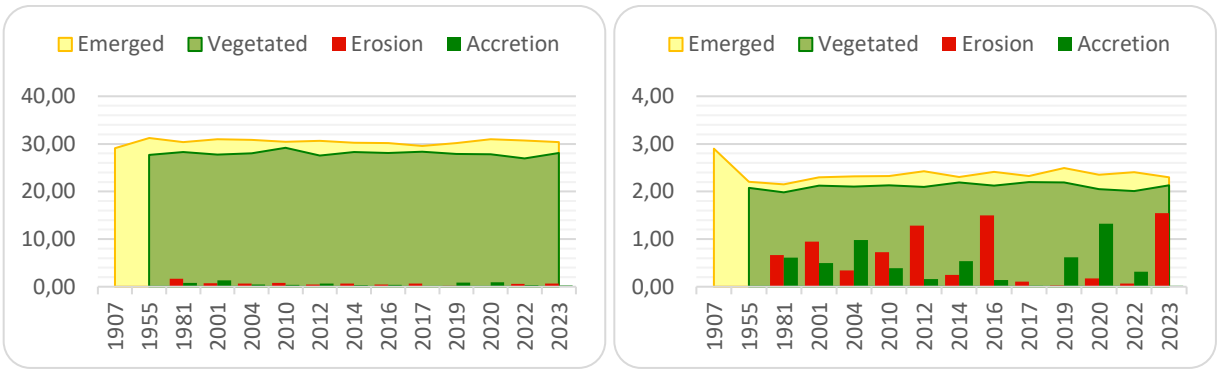

FIGURE 6. Surfaces (ha) of stable motu: Honu'ea (left) and Aie (right)

Aie is a unique case, with a coral debris spire that can be partially or fully submerged depending on the lagoon's water level. As a result, the emerged surface of this spire (detected with DDWI) can vary significantly between two dates compared to the emerged surfaces of the *motu*. As an example, in 2010, the emerged surface of this debris spire is 2.27 ha when the *motu's* emerged surface is 2.32 ha.

Thus, significant variation in erosion and accretion is visible in the diachronic surface analysis (FIGURE 6 right). To avoid giving the false impression that *Aie* is an unstable *motu*, the spire surface has not been included in the emerged surfaces count, as it is one of the most stable in Tetiaroa.

The 1907 surface methodology does not clearly indicate whether this spire was considered, which could explain the differences between 1907 and 1955.

Sandy spires

Almost all stable *motu* have seasonal sandy spires, which are characteristic of the interaction between the lagoon marine currents and the sandy shores.

On Tetiaroa, strong swells arrive mainly from the south (Laurent et al., 2019), explaining the dynamics of the sandy spires of *Aie*, *Honu'ea* and *Rimatu'u* (FIGURE 7 and orange in FIGURE 5), which are highly representative of this phenomenon.

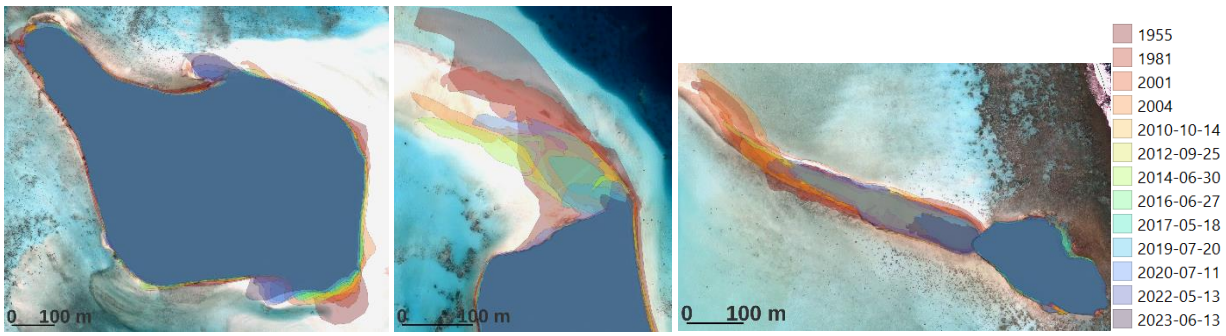

FIGURE 7. Sandy spires of Honu'ea, Rimatu'u and Aie (left to right) 1955-2023

Another type of sandy spires (FIGURE 8 and green in FIGURE 5) are found on the lagoon side of *Tia'ra'aunu*, *Tauvini*, *Hira'a'anae* and *Horoāterā* and is linked to the currents coming from (or towards) the *hoa*. These channels between two nearby *motu* play an important role in filling or emptying the lagoon.

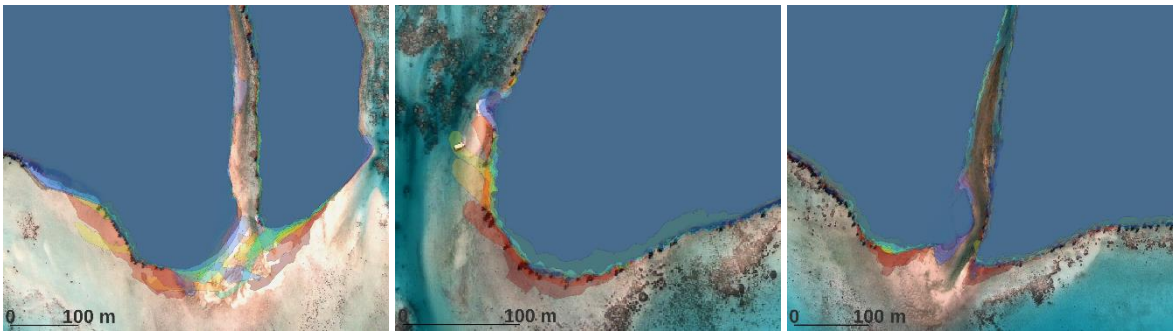

FIGURE 8. Sandy spires of Tia'ra'aunu-Tauvini, Hira'a'anae and Hira'a'anae-Horoāterā (left to right) 1955-2023

3.2. Instable motu

Among all the *motu* in Tetiaroa, three have a highly dynamic geomorphology: *Motu One*, *Tahuna rahi* and *Tahuna iti*. They are all located in an area of sandbanks (red in FIGURE 5), between *Rimatu'u* and *Reiono* in the south of the atoll.

These sand-based islets are stabilized by vegetation until a major climatic event, such as a tropical cyclone or swell, erodes them. The most notable example is *Motu One*, which disappeared between 1955 and 1981, merging with *Rimatu'u* to form a brackish-water lagoon.

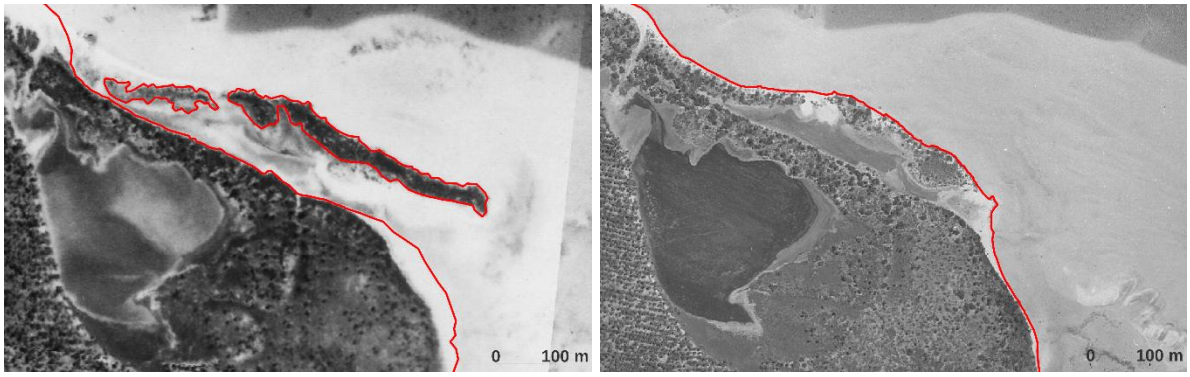

FIGURE 9. Motu One in 1955 (left) and in 1981 (right) – red line is shoreline

The other two sand-based *motu* in the sandbank area are *Tahuna rahi* and *Tahuna iti*. In Tahitian, *tahuna* means sand accumulation, *rahi* means large and *iti* means small.

Tahuna rahi, which, according to toponymy, was the larger of the two *motu*, had almost the same surface area as *Tahuna iti* in 1907 and 1955. However, it underwent severe erosion between 1955 and 2001 (FIGURE 10 left), with its surface divided by a factor of five in less than 50 years.

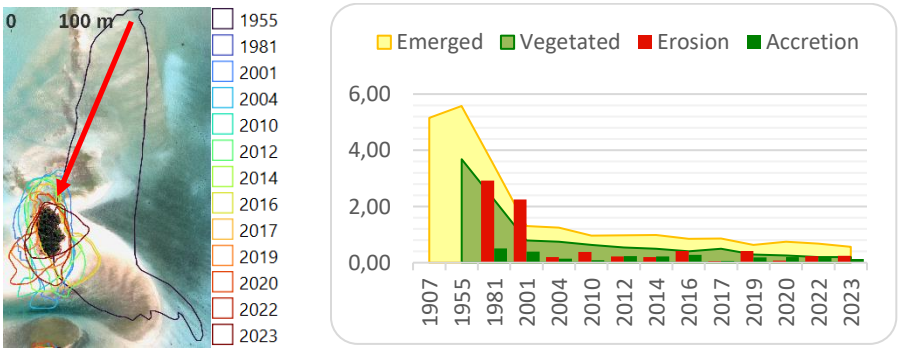

FIGURE 10. Tahuna rahi 1955-2023 shorelines (left) and their surfaces evolutions in ha (right)

Tahuna iti, also known as the "Bird Island" in tourism due to its large bird colony, has also experienced significant erosion but also significant accretion since 1955, resulting in a relatively stable surface area (FIGURE 11 right). Despite this stability, *Tahuna iti* is moving strongly westwards and began merging with *Rimatu'u* in 2024 (FIGURE 12), following a similar fate as *Motu One*.

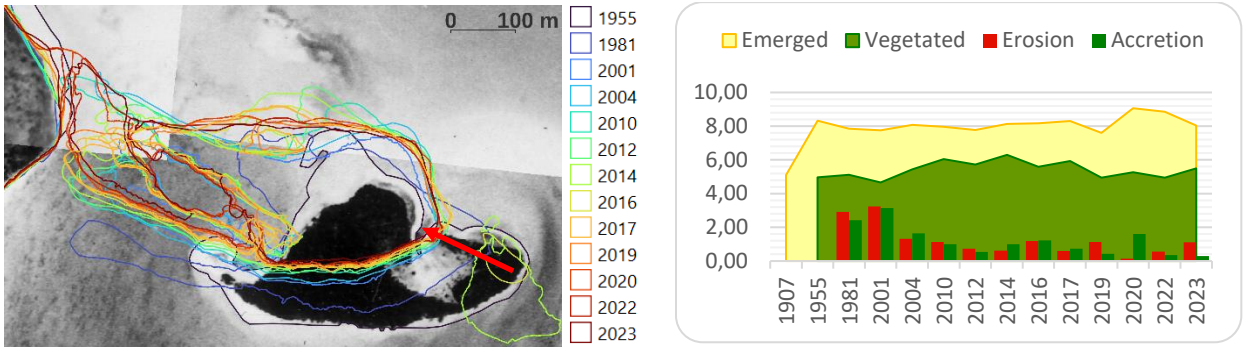

FIGURE 11. Tahuna iti shorelines (left) and surface evolution in ha (right) 1955-2023

FIGURE 12. Tahuna iti dGPS shoreline (red line) in March 2024 (background 2022 Pléiades)

4. Discussions

4.1. Are big motu more stable than small ones?

(Duvat, 2019) indicates that no *motu* larger than 10 ha has decreased in size among the 709 *motu* studied in 30 atolls in the Pacific and Indian oceans over the last few decades.

On Tetiaroa (FIGURE 13), all *motu* with a total surface area greater than 10 ha are effectively stable, and the most dynamic *motu* (*Motu One*, *Tahuna iti* and *Tahuna rahi*) are smaller than 10 ha.

However, three *motu* of less than 10 ha are very stable (*Aie*, *Ahuroa* and *Tauvini*), and contradict this hypothesis. It would therefore be more accurate to say that in the case of Tetiaroa, *motu* with

a rocky base are more stable than sandy *motu*. This hypothesis has yet to be confirmed by geological analysis of the *motu*'s structural foundations.

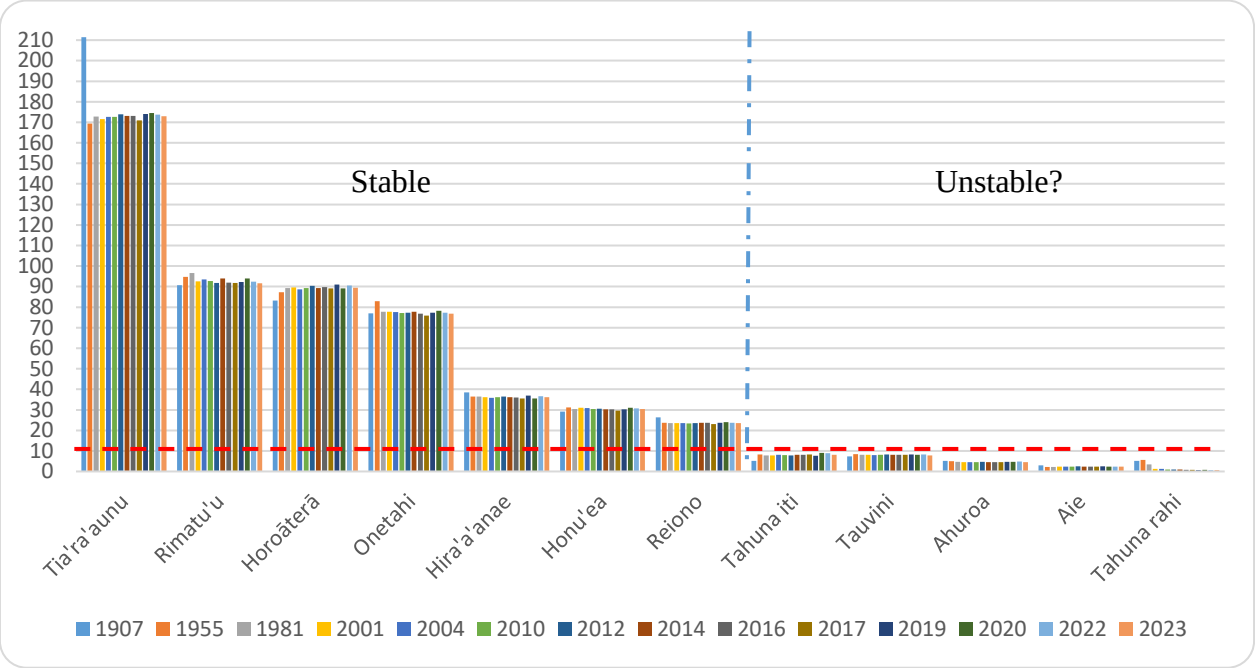

FIGURE 13. Motu emerged surfaces (ha) - 1955-2023

4.2. Historic accretion areas

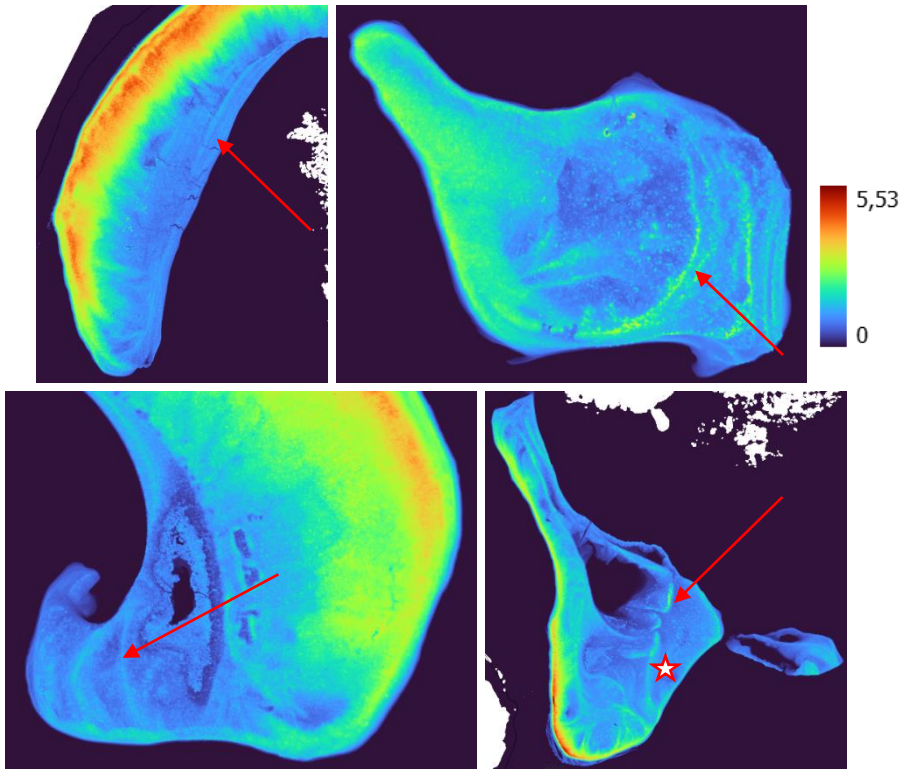

FIGURE 14. 2017 lidar DTM of Tia'ra'aunu, Honu'ea, Horoāterā and Rimatu'u-Tahuna iti (top-left to bottom-right), red arrows show ancient accretions areas, red star shows archeological site

The 2017 lidar data produced a 30 cm digital terrain model of the atoll (Gruen et al., 2017). These data are very useful for detecting and highlighting ancient accretion zones on the Tetiaroa *motu*.

Four *motu* show distinctive marks of ancient accretions (red arrows in FIGURE 14): (i) *Tia'ra'aunu* on the lagoon side, (ii) southeast of *Honu'ea*, where it receives sediments from nearby sandbanks, (iii) *Horoātera* with its sandy spires that created a calm, shallow zone in the lagoon (known as a shark nursery) and probably the former freshwater lake, and (iv) southeast of *Rimatu'u* which receives sediments from the *Tahuna iti* and *Tahuna rahi* sandbanks.

Interestingly, these four motu, which show evidence of ancient accretion, have been considered stable since 1907, according to the results of this study. Archaeological sites, discovered on the eastern side of Rimatu'u (red star in FIGURE 14), indicate that accretions are at least as old as these archaeological sites. These have not yet been formally dated but are estimated to date from the 16th to the 19th century, validating the natural and very ancient aspect of this accretion process.

4.3. Climate change impact on Tetiaroa's motu?

The potential impacts of global warming and induced climate change on the atolls of French Polynesia are of two types: (i) sea level rise has been estimated at an average of 3 mm per year since the 1950's in French Polynesia (Becker et al., 2012), *i.e.* 20 cm between 1955 and 2023. (ii) Climate change is generally associated with an increase in the occurrence and intensity of extreme weather events (tropical cyclones, storms and induced swells). However, (Walsh et al., 2012) indicate that the changes in the frequency of very intense tropical cyclones (cat. 4 and 5) are not uniform on the globe. The frequency will increase in most regions, but will decrease in the South Pacific, among others.

Tetiaroa is, to this day, the only atoll in French Polynesia with a 68-year database of aerial and satellite images, which can be used to assess the impact of climate change on its *motu* shoreline. This database comprises only 13 images, and the sampling rate (FIGURE 15) is not homogeneous over the entire period: 26 years elapsed between the first image and the second, 20 years before the third, and regular imaging only began in 2010, with images every one or two years. While the current statistics may not be significant, they remain to be validated with additional data.

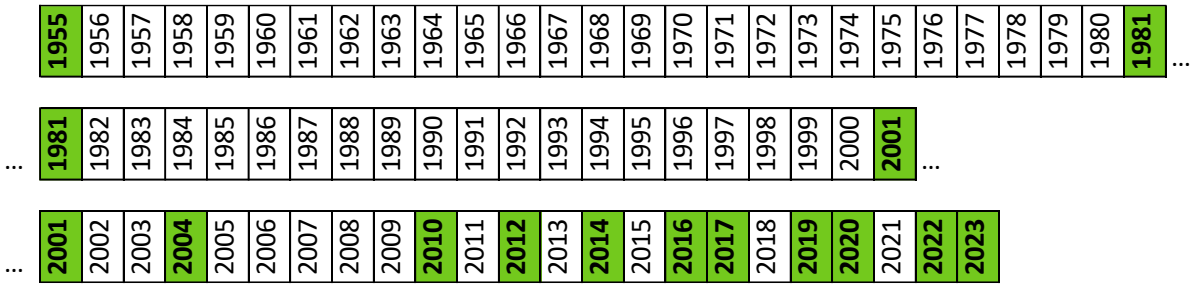

FIGURE 15. Aerial and satellite images timeline (available data in green)

The image database and derived indexes: surface/erosion/accretion and centroid movement show that stable *motu* have undergone very little change since 1955 (and since 1907). These stable *motu* have clearly not yet been affected by the consequences of climate change, in particular sea-level rise, which should be specifically observed.

On the other hand, the unstable *motu* have been constantly evolving throughout the observation period, suggesting that their changes are not necessarily indicative of climate change impacts. Moreover, the most significant changes occurred before 1981, prior to the acceleration of climate change. Therefore, to date, the changes observed on Tetiaroa's shorelines do not appear to be

directly correlated with climate change, but rather seem to result from episodic natural phenomena such as strong swells and tropical cyclones. However, the potential influence of climate change cannot be entirely ruled out.

One of the consequences of global warming is an increase in the frequency and intensity of extreme weather events. According to the IPCC's latest report (Lee and Romero, 2023), there is no definitive evidence that the zones of the South Pacific prone to cyclogenesis and tropical cyclone activity will remain unchanged in the future, it is also uncertain whether there will be an increase in the frequency of tropical cyclones in French Polynesia. Thus, we cannot conclusively state that climate change will lead to more tropical cyclones in the region. However, some experts also predict that tropical cyclone intensity will increase in the future (Knutson et al., 2021). If this proves true, the impact on the *motu* of Tetiaroa could be significant, as the cyclonic swell induced by a single powerful tropical cyclone could lead to radical changes in the atoll's geomorphology.

5. Outlooks and conclusions

Continued monitoring of Tetiaroa's shoreline will document the natural behavior of a pristine tropical atoll over a long period and assess the impact of future extreme climatic events on the *motu*'s geomorphology.

The database will therefore continue to be enriched by very high-resolution satellite images (ideally every one or two years) and dGPS missions along the shoreline (several times a year). These data will enable us to monitor the shoreline's evolution in the context of global warming.

Our study will be improved by (i) setting up a drone protocol to monitor beach scarps, (ii) considering the seasonality of erosion/accretion of seasonal sandy spires and sand-based *motu* through regular dGPS campaigns, (iii) detecting and monitoring sandbanks and their dynamics on satellite images and dGPS campaigns, (iv) in the long term, *motu* dynamics should be linked to lagoon bathymetry and currents.

All the analyses and conclusions reported here must consider that Tetiaroa is a small, closed atoll, with minimal anthropogenic activity. Therefore, it may not fully represent all atolls in French Polynesia, and it is especially different from the anthropized high islands such as Tahiti, Moorea, Raiatea.

In this context, few impacts of global warming are visible on the Tetiaroa atoll as of 2024, considering the period from 1907 to 2023. Although a few *motu* are indeed changing, this is a natural phenomenon that began before the onset of global warming.

However, the intensification of climate change, characterized by more extreme weather events, could drastically accelerate the movement of unstable *motu* and potentially impact even stable *motu*. Therefore, continued monitoring is essential.

Bibliography

Abdelhady, H.U., Troy, C.D., Habib, A., Manish, R., 2022. A Simple, Fully Automated Shoreline Detection Algorithm for High-Resolution Multi-Spectral Imagery. Remote Sensing 14, 557.

Albert, S., Leon, J.X., Grinham, A.R., Chruch, J.A., Gibbes, B.R., Woodroffe, C.D., 2016. Interactions between sea-level rise and wave exposure on reef island dynamics in the Solomon Islands. Environmental Research Letters.

Becker, M., Meyssignac, B., Letetrel, C., Llovel, W., Cazenave, A., Delcroix, T., 2012. Sea level variations at tropical Pacific islands since 1950. Global and Planetary Change 80-81:85-98.

Boak, E.H., Turner, I.L., 2005. Shoreline Definition and Detection: A Review. Journal of Coastal Research 21 688–703.

Botella, A., 2015. Past and Future Sea-Level Changes in French Polynesia. University of Ottawa.

Canavesio, R., 2019. Distant swells and their impacts on atolls and tropical coastlines. The example of submersions produced by lagoon water filling and flushing currents in French Polynesia during 1996 and 2011 mega swells. Global and Planetary Change 116–126.

Dumas, F., Le Gendre, R., Thomas, Y., Andrefouet, S., 2012. Tidal flushing and wind driven circulation of Ahe atoll lagoon (Tuamotu Archipelago, French Polynesia) from in situ observations and numerical modelling. Marine Pollution Bulletin 425–440.

Duvat, V.K.E., 2019. A global assessment of atoll island planform changes over the past decades. WIREs Clim Change 10.

Gao, B.-C., 1996. NDWI—A normalized difference water index for remote sensing of vegetation liquid water from space. Remote Sensing of Environment 257–266.

Gruen, A., Tao Guo, Serkan Ural, Matthias Troyer, Sultan Kocaman, 2017. DSM/DTM-related investigations of the Moorea Avatar project. Presented at the Asian Conference on Remote Sensing, New Delhi, India.

Knutson, T.R., Chung, M.V., Vecchi, G., SUN, J., Hsieh, T.-L., Smith, A.J.P., 2021. ScienceBrief Review: Climate change is probably increasing the intensity of tropical cyclones. Critical Issues in Climate Change Science.

Kriegler, F.J., Malila, W.A., Nalepka, R.F., Richardson, W., 1969. Preprocessing transformations and their effect on mutispectral recognition. Remote Sensing of Environment VI 97–132.

Laurent, V., Maamaatuaiahutapu, K., Brodien, H., Lombardo, S., Tardy, M., Varney, P., 2019. Atlas climatologique de la Polynésie française, Météo France, Délégation interrégionale de Polynésie française. ed.

Le Cozannet, G., Garcin, M., Petitjean, L., Cazenave, A., Becker, M., Meyssignac, B., Walker, P., Devilliers, C., Le Brun, O., Lecacheux, S., Bailles, A., Bulteau, T., Yates, M., Wöppelmann, G., 2013. Exploring the relation between sea level rise and shoreline erosion using sea level reconstructions: An example in French Polynesia. Presented at the 12th International Coastal Symposium, Journal of Coastal Research, pp. 2137–2142.

Lee, H., Romero, J., 2023. Climate Change 2023: Synthesis Report. Contribution of Working Groups I, II and III to the Sixth Assessment Report of the Intergovernmental Panel on Climate Change., IPCC. IPCC, Geneva, Switzerland.

Paris, P., Mitasova, H., 2014. Barrier Island Dynamics Using Mass Center Analysis: A New Way to Detect and Track Large-Scale Change. IJGI 49–65.

Pillet, V., 2020. Détection et attribution des changements morphologiques côtiers récents en milieu insulaire tropical (Polynésie française, Caraïbe). NNT : 2020LAROS019.

Stoll, B., Longine, M., 2019. Géomorphologie à Tetiaroa : Prémices d'un observatoire de données scientifiques et environnementales. Presented at the SAGEO, Clermont-Ferrand.

Stoll, B., tuheiava, P., Badie, M., De Oliveira, L., 2023. Cartographie lidar des biotopes terrestres, marins et intertidaux de l'atoll de Tetiaroa. Presented at the SAGEO, Québec.

Walsh, K.J., McInnes, K.L., McBride, J.L., 2012. Climate change impacts on tropical cyclones and extreme sea levels in the South Pacific—A regional assessment. Global and Planetary Change 149-164.

Yates, M.L., Le Cozannet, G., Garcin, M., Salaï, E., Walker, P., 2013. Multidecadal Atoll Shoreline Change on Manihi and Manuae, French Polynesia. Journal of Coastal Research 289 870–882.

Annexes:

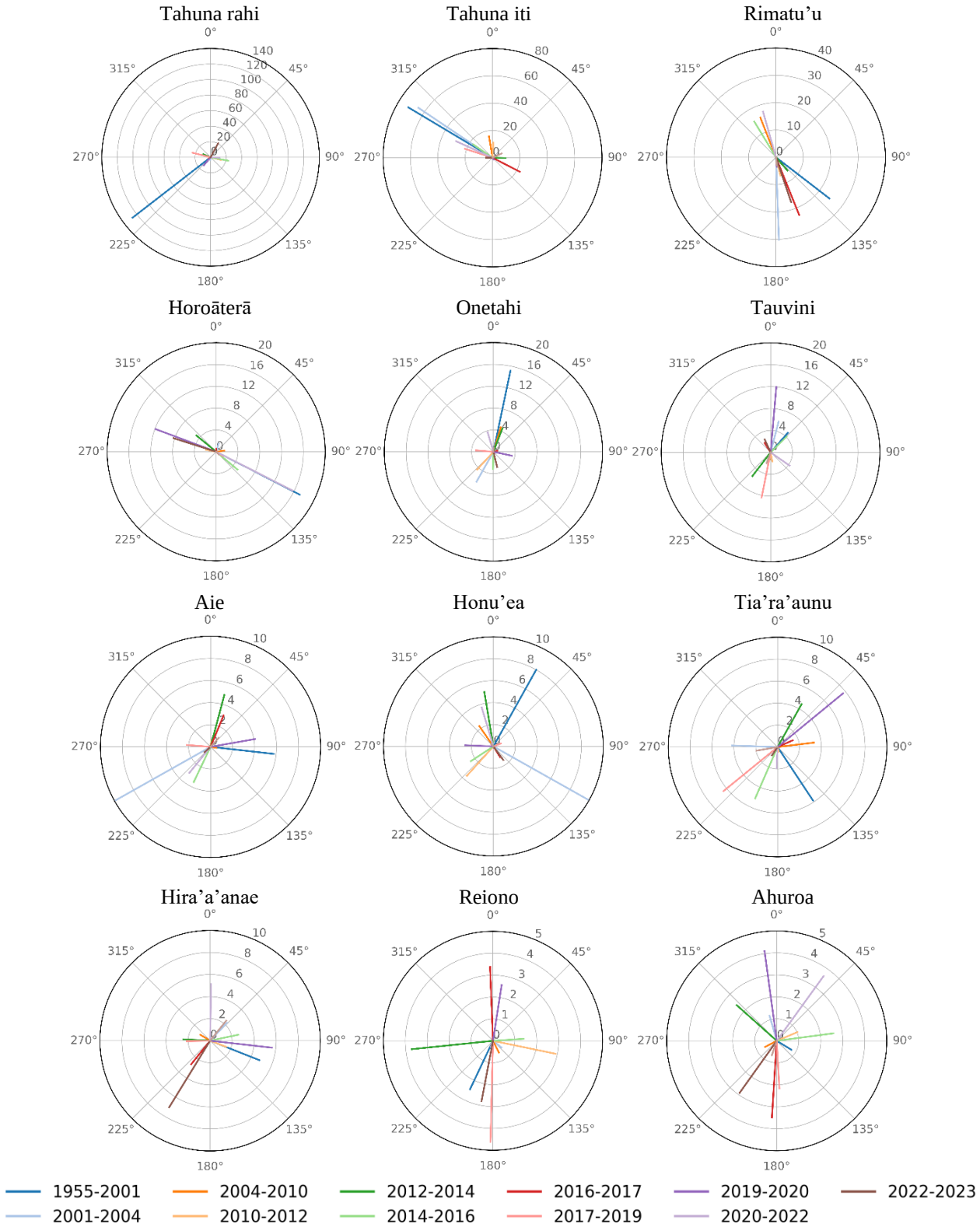

FIGURE 16. Tetiaroa motu centroid movements

Aie	1907	1955	1981	2001	2004	2010	2012	2014	2016	2017	2019	2020	2022	2023
Emerged	2.90	2.20	2.15	2.30	2.31	2.33	2.43	2.31	2.41	2.32	2.49	2.35	2.40	2.30
Vegetated		2.08	1.98	2.13	2.10	2.13	2.10	2.19	2.12	2.20	2.19	2.05	2.01	2.13
Erosion			0.66	0.95	0.34	0.73	1.28	0.25	1.50	0.11	0.03	0.17	0.07	1.55
Accretion			0.61	0.50	0.98	0.39	0.16	0.54	0.14	0.02	0.62	1.32	0.31	0.02
Ahuroa	1907	1955	1981	2001	2004	2010	2012	2014	2016	2017	2019	2020	2022	2023
Emerged	5.20	4.93	4.74	4.60	4.55	4.60	4.65	4.56	4.60	4.59	4.71	4.62	4.77	4.59
Vegetated		4.93	4.74	4.60	4.53	4.57	4.46	4.56	4.41	4.57	4.36	4.33	4.35	4.48
Erosion			0.28	0.17	0.11	0.07	0.07	0.17	0.08	0.10	0.06	0.18	0.03	0.18
Accretion			0.10	0.02	0.06	0.12	0.12	0.08	0.12	0.09	0.19	0.08	0.18	0.00
Hira'a'anae	1907	1955	1981	2001	2004	2010	2012	2014	2016	2017	2019	2020	2022	2023
Emerged	38.45	36.52	36.49	36.21	35.86	36.14	36.44	36.12	35.98	35.48	36.99	35.60	36.61	36.10
Vegetated		33.45	34.87	34.47	34.38	33.17	33.37	33.86	34.08	34.75	33.98	33.21	33.75	33.95
Erosion			0.54	0.62	0.41	0.10	0.32	0.63	0.44	0.67	0.13	1.54	0.21	0.63
Accretion			0.53	0.34	0.06	0.37	0.65	0.27	0.30	0.17	1.64	0.15	1.23	0.11
Honu'ea	1907	1955	1981	2001	2004	2010	2012	2014	2016	2017	2019	2020	2022	2023
Emerged	29.10	31.23	30.36	31.01	30.81	30.43	30.61	30.25	30.17	29.55	30.19	30.98	30.71	30.36
Vegetated		27.70	28.30	27.73	28.05	29.18	27.58	28.30	28.10	28.37	27.88	27.81	26.97	28.09
Erosion			1.66	0.70	0.64	0.80	0.49	0.66	0.47	0.69	0.22	0.12	0.59	0.64
Accretion			0.79	1.35	0.45	0.42	0.67	0.30	0.38	0.07	0.86	0.91	0.32	0.29
Motu One	1907	1955	1981	2001	2004	2010	2012	2014	2016	2017	2019	2020	2022	2023
Emerged	3.10	2.12												
Vegetated		2.12												
Erosion			1.25											
Accretion														
Onetahi	1907	1955	1981	2001	2004	2010	2012	2014	2016	2017	2019	2020	2022	2023
Emerged	76.90	82.88	77.73	77.74	77.57	77.11	77.26	77.71	76.87	75.92	77.30	78.29	77.27	76.84
Vegetated		73.79	71.63	71.35	72.08	74.26	72.87	73.90	73.91	74.06	73.45	74.12	72.35	73.80
Erosion			5.55	1.36	0.81	0.81	0.51	0.26	1.00	1.10	0.16	0.29	1.24	0.64
Accretion			0.39	1.37	0.64	0.35	0.67	0.71	0.16	0.15	1.54	1.28	0.22	0.21
Horoāterā	1907	1955	1981	2001	2004	2010	2012	2014	2016	2017	2019	2020	2022	2023
Emerged	83.20	87.31	89.30	89.59	88.65	89.24	90.45	89.31	89.71	89.10	90.97	89.15	90.60	89.48
Vegetated		82.42	84.01	83.46	83.09	83.69	84.00	84.35	84.55	85.02	84.39	83.70	84.09	84.92
Erosion			0.86	0.95	1.16	0.20	0.23	1.38	0.38	0.86	0.29	2.63	0.39	1.23
Accretion			2.85	1.24	0.22	0.80	1.39	0.29	0.77	0.25	2.16	0.80	1.83	0.13
Reiono	1907	1955	1981	2001	2004	2010	2012	2014	2016	2017	2019	2020	2022	2023
Emerged	26.30	23.67	23.57	23.47	23.57	23.45	23.50	23.72	23.67	23.11	23.71	23.94	23.74	23.46
Vegetated		21.91	22.00	22.09	21.98	22.22	22.26	22.31	22.46	22.42	22.24	22.28	22.13	22.25
Erosion			0.20	0.15	0.08	0.17	0.21	0.20	0.21	0.60	0.06	0.07	0.29	0.33
Accretion			0.09	0.07	0.18	0.04	0.27	0.42	0.16	0.03	0.67	0.30	0.08	0.05
Rimatu'u	1907	1955	1981	2001	2004	2010	2012	2014	2016	2017	2019	2020	2022	2023
Emerged	90.70	94.75	96.56	92.55	93.46	92.69	91.83	93.99	91.87	91.81	92.28	93.99	92.43	91.62
Vegetated		86.05	89.60	86.50	87.69	88.12	87.46	87.97	88.28	88.40	87.31	87.48	86.97	88.45
Erosion			3.45	4.38	0.47	1.21	1.36	0.25	2.33	0.59	0.47	0.23	1.73	0.89
Accretion			4.39	0.37	1.38	0.44	0.51	2.41	0.21	0.53	0.93	1.94	0.16	0.09
Tahuna Iti	1907	1955	1981	2001	2004	2010	2012	2014	2016	2017	2019	2020	2022	2023
Emerged	5.10	8.33	7.85	7.75	8.08	7.96	7.78	8.14	8.18	8.31	7.60	9.06	8.86	8.04
Vegetated		4.96	5.11	4.66	5.43	6.04	5.72	6.30	5.59	5.92	4.95	5.27	4.95	5.50
Erosion			2.91	3.24	1.31	1.13	0.72	0.62	1.19	0.60	1.13	0.15	0.56	1.11
Accretion			2.43	3.14	1.65	1.01	0.54	0.99	1.23	0.74	0.42	1.61	0.36	0.29
Tahuna Rahi	1907	1955	1981	2001	2004	2010	2012	2014	2016	2017	2019	2020	2022	2023
Emerged	5.15	5.58	3.44	1.31	1.25	0.96	0.97	0.99	0.85	0.86	0.63	0.75	0.68	0.56
Vegetated		3.68	2.23	0.79	0.75	0.63	0.54	0.49	0.41	0.49	0.29	0.26	0.20	0.21
Erosion			2.92	2.25	0.20	0.38	0.23	0.20	0.41	0.05	0.42	0.08	0.23	0.24
Accretion			0.51	0.39	0.14	0.09	0.24	0.22	0.28	0.06	0.19	0.20	0.16	0.13
Tauvini	1907	1955	1981	2001	2004	2010	2012	2014	2016	2017	2019	2020	2022	2023
Emerged	7.40	8.41	8.09	8.09	7.94	8.10	8.29	8.08	8.17	8.16	8.24	8.08	8.20	7.88
Vegetated		7.51	7.60	7.34	7.27	7.20	7.25	7.44	7.50	7.46	7.09	7.23	7.06	7.18
Erosion			0.49	0.25	0.23	0.09	0.17	0.34	0.15	0.25	0.28	0.39	0.14	0.32
Accretion			0.17	0.26	0.07	0.26	0.36	0.13	0.24	0.24	0.35	0.23	0.25	0.00
Tia'ra'aunu	1907	1955	1981	2001	2004	2010	2012	2014	2016	2017	2019	2020	2022	2023
Emerged	211.5	169.41	172.72	171.61	172.65	172.56	173.93	173.05	173.14	170.88	174.08	174.45	173.79	172.99
Vegetated		163.78	163.70	164.09	164.24	162.80	163.92	164.40	164.96	165.29	164.65	164.94	164.03	165.99
Erosion			0.98	2.27	0.16	0.69	0.50	1.73	0.65	2.32	0.10	0.96	1.45	0.95
Accretion			4.30	1.16	1.20	0.60	1.88	0.85	0.74	0.06	3.30	1.33	0.80	0.15

TABLE 2. Emerged, vegetated, erosion and accretion surfaces (ha) for each motu